

Designing a Fast and Flexible Quantum State Simulator

Saveliy Yusufov, Charlee Stefanski, and Constantin Gonciulea

Wells Fargo

This paper describes the design and implementation of Spinoza, a fast and flexible quantum simulator written in Rust. Spinoza simulates the evolution of a quantum system’s state by applying quantum gates, with the core design principle being that a single-qubit gate applied to a target qubit preserves the probability of pairs of amplitudes corresponding to measurement outcomes that differ only in the target qubit. Multiple strategies are employed for selecting pairs of amplitudes, depending on the gate type and other parameters, to optimize performance. Specific optimizations are also implemented for certain gate types and target qubits.

Spinoza is intended to enable the development of quantum computing solutions by offering developers a simple, flexible, and fast tool for classical simulation. In this paper we provide details about the design and usage examples. Furthermore, we compare Spinoza’s performance against several other open-source simulators to demonstrate its strengths.

1 Introduction

Several types of users, including researchers, software developers, and students, use quantum simulators to experiment with quantum algorithms and circuits in a controlled environment without needing access to actual quantum hardware. Classical simulation is also an essential tool for analyzing results from quantum hardware. Classical simulators are essential in the Noisy Intermediate-Scale Quantum (NISQ) era since currently available quantum devices have limited capacity for depth, circuit complexity, and high error rates [1]. By using classical simulators, researchers can continue to develop and test quantum algorithms despite these limitations. However, simulating quantum computers with classical computers is a difficult task. The computational resources and simulation time increases exponentially with the size of the quantum system (qubits). This complexity also demonstrates the potential utility and promise of quantum computing to perform tasks beyond the reach of classical computers.

Spinoza is designed to fulfill the need for a

quantum simulator that is flexible and efficient for use in several different environments, including personal computers. Spinoza offers all the essential capabilities for quantum algorithm development with both Rust and Python interfaces. In standard benchmarks, Spinoza is one of the fastest simulators when compared with several other open-source simulators.

This paper consists of the following: In Section 2 discusses the preliminary concepts imperative to the design and implementation of Spinoza. Section 3 provides an overview of the design. Section 4 details the implementation in Rust and in addition to the Python module. Section 5 discusses the optimization techniques used in the simulator. Section 6 compares the performance of Spinoza with several existing simulators.



Figure 1: **Baruch Spinoza (1632-1677)** [2] This project is called “Spinoza”, named after Baruch Spinoza, the 17th century Dutch Philosopher.

2 Preliminaries

The state of a quantum system with $n > 0$ qubits can be modeled as a list of amplitudes corresponding to the 2^n possible outcomes of the state measurement in the computational basis. This is typically expressed using Dirac’s ket notation:

$$|\gamma\rangle_n = \sum_{i=0}^{2^n-1} a_i |i\rangle \quad (1)$$

The probability of the outcome corresponding to $|i\rangle$ is $|a_i|^2$, for $i \in \{0, \dots, 2^n - 1\}$, and $\sum_{i=0}^{2^n-1} |a_i|^2 = 1$.

Depending on the context, an outcome can be interpreted as an integer, $i \in \{0, \dots, 2^n - 1\}$, or its

binary string representation, where each digit corresponds to a qubit. For example, a 3-qubit quantum state can be expressed as:

$$|\gamma\rangle_3 = a_0 |000\rangle + a_1 |001\rangle + a_2 |010\rangle + a_3 |011\rangle + a_4 |100\rangle + a_5 |101\rangle + a_6 |110\rangle + a_7 |111\rangle. \quad (2)$$

3 Approach and Design

At the core of the design is the fact that single-qubit gate transformations act on amplitude pairs, preserving the probability of individual pairs. A unified approach for handling target and control qubits allows for an efficient implementation of multi-control transformations. Gate transformations are optimized according to gate type.

Spinoza's implementation of the evolution of the state of a quantum system by applying a (controlled) gate has two steps:

1. Select the pairs of amplitudes that are updated together. Note that for some gates (e.g., Phase gate) only one side of the pair is needed.
2. Apply the gate to update either one or both sides of each such pair.

When a single-qubit gate is applied on a target qubit, $t \in \{0, \dots, n-1\}$, the probability of the two outcomes that differ only in the t position is preserved. We can rewrite the state defined in Eq. 1 by grouping such pairs:

$$|\gamma\rangle_n = \sum_{j=0}^{2^{n-1}-1} (a_{z(j,t)} |z(j,t)\rangle + a_{o(j,t)} |o(j,t)\rangle) \quad (3)$$

where $z(j,t)$ is the $n-1$ digit binary expansion of j with 0 inserted in position t , and $o(j,t)$ is the $n-1$ digit binary expansion of j with 1 inserted in position t .

For example, given a 3-qubit state, $|\gamma\rangle_3$ (as defined in Eq 2), a single-qubit gate applied to the middle qubit (i.e., $t = 1$) would yield the following pairs of outcomes:

$$\begin{aligned} z(0,1) &= 0 = 000_2 \text{ and } o(0,1) = 2 = 010_2 \\ z(1,1) &= 1 = 001_2 \text{ and } o(1,1) = 3 = 011_2 \\ z(2,1) &= 4 = 100_2 \text{ and } o(2,1) = 6 = 110_2 \\ z(3,1) &= 5 = 101_2 \text{ and } o(3,1) = 7 = 111_2 \end{aligned}$$

Considering these outcome pairs, we can define the state in Eq. 2 by pair groupings:

$$\begin{aligned} |\gamma\rangle_3 &= (a_0 |000\rangle + a_2 |010\rangle) + \\ & (a_1 |001\rangle + a_3 |011\rangle) + \\ & (a_4 |100\rangle + a_6 |110\rangle) + \\ & (a_5 |101\rangle + a_7 |111\rangle) \end{aligned}$$

3.1 Pair Selection

When a single-qubit gate is applied to a target qubit, it changes the amplitudes and corresponding probabilities of measuring 0 or 1 for that qubit. The effect of the gate application can be understood as preserving the probability of pairs of outcomes that differ only in the target qubit, as formalized in Eq. 3.

Four strategies for selecting pairs are described below. For each strategy, we use the example of a 3-qubit quantum state and the middle qubit as the target. Namely, we set $t = 1$.

The list of binary expressions of the outcomes with 0 in the target position is:

$$[000, 001, 100, 101],$$

Similarly, the list of corresponding outcomes with 1 in the target position is:

$$[010, 011, 110, 111].$$

3.1.1 Strategy 0: Traverse and Recognize

We start with the list of all possible outcomes represented as binary strings:

$$[000, 001, 010, 011, 100, 101, 110, 111].$$

For a system with $n > 0$ qubits, we traverse the list, and we check if an outcome $i \in \{0, \dots, 2^n - 1\}$ has 1 in the target qubit position, $t \in \{0, \dots, n-1\}$. In code, the condition can be implemented as the boolean expression $(i \gg t) \& 1$.

We have also found three other strategies that offer better performance depending on the gate. They have the following observation in common:

Observation 3.1. *For a given prefix-suffix combination $j \in \{0, \dots, 2^{n-1}\}$, target position $t \in \{0, \dots, n-1\}$, if q and r are the quotient and remainder, respectively, of dividing j by 2^t , (i.e., $j = q \cdot 2^t + r$, with $r \in \{0, \dots, 2^t - 1\}$), then*

$$\begin{aligned} z(j,t) &= 2q \cdot 2^t + r \\ o(j,t) &= (2q + 1) \cdot 2^t + r \end{aligned} \quad (4)$$

The quotient q and the remainder r are the prefix and suffix with respect to the target position t in the binary representation of the outcome corresponding to j .

3.1.2 Strategy 1: Group and Traverse

We start with the list of all possible measurement outcomes represented as binary strings. We split the list in chunks of size 2^t . In this example $t = 1$, so the chunk size is $2^t = 2$. The chunks alternate between containing 2^t items with 0 in the target position,

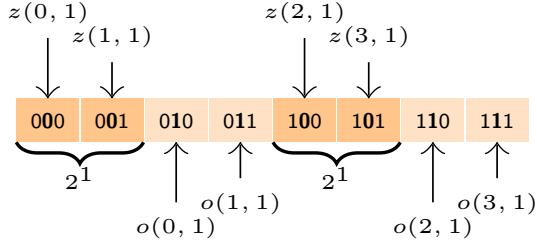


Figure 2: Visualization of the group and traverse strategy of pair selection for a 3-qubit state with $t = 1$.

and 2^t items with 1 in the target position. Figure 2 illustrates this strategy.

This strategy is an optimization of Strategy 0, (see Section 3.1.1). We leverage the fact that within a given chunk of length 2^t , the target qubit does not change. This strategy is especially useful when each side of the pair can be updated independent of the other side. In the case of the R_z -gate, this strategy provides significant optimization opportunities, which are discussed in Section 5.

3.1.3 Strategy 2: Concatenate Prefix, Target and Suffix

Strategy 2 requires us to generate the prefix, append the target, and finally generate the suffix. The prefix and suffix are the possible values expressed with the qubits before and after the target qubit, respectively. For this example, the possible prefix values are 0 and 1.

For each possible prefix, we append 0 or 1 in the target position:

00 01
10 11.

The possible generated suffixes are 0 and 1. Each possible suffix is appended to each combination of prefix and target:

000 010
001 011
100 110
101 111

With the same notations as in Observation 3.1, this strategy can use two nested loops on q and r that generate the outcomes that have 0 or 1 in the target position as in Eq. 4. This strategy is illustrated in Figure 3.

3.1.4 Strategy 3: Insert Target

Strategy 3 requires us to generate the prefix-suffix combinations, and then insert the target. The possible prefix-suffix combinations are:

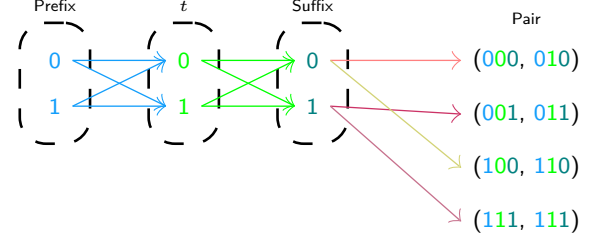


Figure 3: Example of generating pairs for a 3-qubit state with target qubit set to 1 (i.e., $t = 1$) for generating pairs using strategy 2; generating the possible prefixes, appending 0 or 1 in the target position, then generating the possible suffixes and appending each to each prefix-target combination.

00 01 10 11.

To generate the pair items with 0 in the target position, we insert 0 into the target position, in this case the middle:

000 001 100 101.

To generate the corresponding pair items with 1 in the target position, we insert 1 into the target position of the same prefix-suffix combination:

010 011 110 111.

This strategy is illustrated in Figure 4.

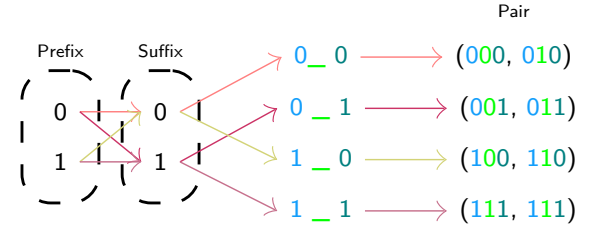


Figure 4: Example of generating pairs for a 3-qubit state with target qubit 1 (i.e., $t = 1$) for generating pairs using strategy 3—generating prefix-suffix combinations, and then inserting 0 or 1 in the target position.

This strategy can be easily generalized for handling control qubits.

If $n > 0$ is the number of binary digits of the possible outcomes, then this strategy can be represented with the formula below:

Lemma 3.2. *With the same notations as in Observation 3.1, the following closed-form expressions can be used for pair generation:*

$$z(j, t) = j + ((j \gg t) \ll t)$$

$$o(j, t) = j + (((j \gg t) + 1) \ll t)$$

Proof.

$$\begin{aligned}
z(j, t) &= 2(q2^t) + r \\
&= q2^t + q2^t + r \\
&= j + q2^t \\
&= j + (q \ll t) \\
&= j + ((j \gg t) \ll t)
\end{aligned}$$

$$\begin{aligned}
o(j, t) &= 2^t + z(j, t) \\
&= j + (((j \gg t) + 1) \ll t)
\end{aligned}$$

□

Spinoza is implemented such that each gate uses the pair strategy that is optimized for the application of that gate.

3.2 Amplitude Update

The method of pairing outcomes and amplitudes is at the core of the simulator's implementation of single-qubit gate applications. Assume a single-qubit gate is represented in matrix form:

$$g = \begin{bmatrix} g_{00} & g_{01} \\ g_{10} & g_{11} \end{bmatrix}.$$

Let U_g be the unitary operator corresponding to this single-qubit gate, then its application to a n -qubit quantum state $|\gamma\rangle_n$, as defined in Eq. 1, yields

$$U_g |\gamma\rangle_n = \sum_{j=0}^{2^{n-1}-1} (b_{z(j,t)} |z(j,t)\rangle_n + b_{o(j,t)} |o(j,t)\rangle_n)$$

where

$$\begin{bmatrix} b_{z(j,t)} \\ b_{o(j,t)} \end{bmatrix} = \begin{bmatrix} g_{00} & g_{01} \\ g_{10} & g_{11} \end{bmatrix} \begin{bmatrix} a_{z(j,t)} \\ a_{o(j,t)} \end{bmatrix}.$$

Therefore,

$$\begin{aligned}
U_g |\gamma\rangle_n &= \sum_{j=0}^{2^{n-1}-1} ((g_{00}a_{z(j,t)} + g_{01}a_{o(j,t)}) |z(j,t)\rangle_n \\
&\quad + (g_{10}a_{z(j,t)} + g_{11}a_{o(j,t)}) |o(j,t)\rangle_n).
\end{aligned}$$

Note that qubits are indexed from the right. Also, to simplify understanding, sometimes we do not distinguish between a gate and its unitary.

3.3 Controlled Gate Transformations

When one or more control qubits are part of a gate transformation, only the amplitude pairs corresponding to outcomes that have 1 in the control positions are being processed.

By default, Spinoza uses the insertion strategy (i.e., Strategy 3), for controlled gate applications.

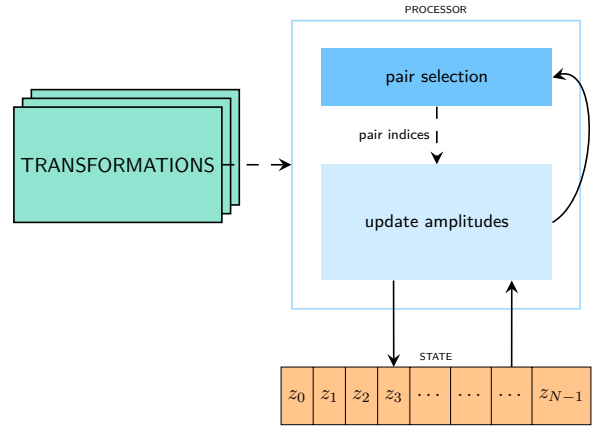


Figure 5: Visualization of the serial implementation of the simulator. Transformations are passed to the single processor in order, and the amplitudes of the state are updated in pairs.

4 Implementation

4.1 Using Rust

The exponential growth in run-time for simulating a quantum computer with a classical machine prompts the need for an efficient simulator. Implementing a fast quantum simulator requires the use of a programming language that provides blazingly fast performance, efficient use of memory, and a low level of control. The C and C++ programming languages fit the aforementioned criteria, but with many potential issues that are beyond the scope of this paper. The Rust programming language [3] suffices all the aforementioned requirements for a fast quantum simulator, and Rust brings additional benefits to the table.

The primary benefit of Rust comes from the borrow checker, which helps eliminate memory safety bugs that continue to plague projects written in C and C++. Given the safety guarantees that are enforced by the compiler, project maintainers can spend less time reviewing code submissions.

By implementing the simulator in Rust, quantum computing researchers and quantum software engineers can spend more time adding new functionality and running simulations, and less time verifying correctness of their code.

4.2 Code Structure

4.2.1 Single vs. Double Precision

The implementation discussed and used for all benchmarks (Section 6) in this paper uses double-precision floating-point values (i.e., variable type with 64 bits) for representing the amplitudes of quantum states and the values used for gate transformations. Users should consider using single-precision (i.e., 32 bit) floating-point types for additional performance benefits. Using single

precision allows for more of the state vector to fit into the cache. For the convenience of users, Spinoza can easily be built and installed to use single-precision complex numbers by invoking the `single` feature flag. In our testing, single-precision complex numbers offered a 30% performance improvement. For several use cases, double-precision values may not be required. Note that the use of single-precision complex numbers implies that the state vector only requires half the memory as compared to the amount of memory required when using double-precision complex numbers. Hence, the use of single-precision complex numbers gives users the ability to introduce an extra qubit into their quantum state simulation, at the cost of precision. For example, in the case of 32 qubits, the state vector would require $2^{32} \cdot 128 \approx 68.72$ GB of memory when using double-precision complex numbers. On a machine with only 64 GB of memory, this would lead to page faults, which would dramatically reduce the performance of the simulation. By using single-precision complex numbers, the state vector would only require $2^{32} \cdot 64 \approx 34.36$ GB of memory, which would allow for fast simulation of the quantum state without reducing the number of qubits.

4.2.2 Quantum State Representation

A quantum state can be represented as a vector of complex numbers. In Spinoza, the state is defined as a structure consisting of two vectors of single or double-precision floating-point types—one for real components and one for the imaginary components of each amplitude—and an unsigned one byte integer value n , or the number of qubits represented by the state. The Rust implementation of the state vector data structure used in Spinoza is shown in Appendix A, listing 1. Ostensibly, the state vector can be defined as a single vector of single or double precision complex numbers; however, separating the real and imaginary components into two separate vectors creates opportunities for optimizations that are not possible with a single vector. Specific optimizations that leverage this attribute are discussed in Section 5.2. The same data structure is used for multiple registers of qubits in one quantum circuit.

There is a method for initializing a state vector, which takes an unsigned integer and initializes a state vector to $|0\rangle$. This function is used in the Spinoza example in listing 7 in Appendix B.

4.2.3 Gate Structure

In a general case, a single-qubit gate is defined as an array of four complex numbers. Similar to the amplitudes of a quantum state, each complex number is defined by two single or double precision

floating-point types for the real and imaginary components. While the convention is to define a gate with a two-by-two matrix, a one-dimensional representation offers better memory locality, less memory consumption, and less allocations [4].

For each gate, the most efficient strategy for identifying or generating the pairs is implemented as a method of the gate.

4.2.4 Pairs

Rust implementations for each of the pair selection strategies described in Section 3.1 are in Appendix A, listings 2 through 5. The best performing pair selection strategy for each gate type is used. Furthermore, additional optimizations for pair selection are used in specific cases, depending on the gate type and target qubit. Note that in the current implementation of Spinoza, the traverse and recognize strategy (strategy 0) is not used.

When applying single-qubits gates Y , Z , P , R_y , and U the concatenation strategy (strategy 2) is used for generating the pairs, as shown in Appendix A, listing 4. The group and traverse strategy (strategy 1), as shown in Appendix A, listing 3 is used for applying the R_z gate. When applying the single-qubit gates X , H , and R_x , the concatenation strategy (strategy 2) is also used, with an additional optimization for when the target qubit is 0, which is explained in Section 5.

When applying control and multi-control gate transformations, pair selection strategies can be optimized. For example, a modified version double shift strategy (strategy 3), as shown in Appendix A, listing 6, is only used for controlled gate applications.

4.2.5 Gate Transformation/Amplitude Update

As discussed in Section 3, gate transformations are executed by identifying pairs of amplitudes and updating those amplitudes according to the gate coefficients. In Spinoza, gate transformations can be applied to a state using the functional syntax used in the example in Appendix A listing 3, or using the circuit syntax discussed in the next section. The functional approach gives the developer control and flexibility when designing an algorithm.

4.2.6 Quantum Circuits

Spinoza includes methods that allow for quantum circuit development with a circuit syntax comparable to Qiskit's [5]. Listing 8 in Appendix B defines and executes a quantum circuit using the circuit syntax. Two data structures make up the circuit components: registers and circuits. A `QuantumRegister` is a vector of integers (`usize`) which correspond to indices of a state. A `QuantumCircuit` is a vector of

transformations and a state vector which reflects the register or registers used in the circuit. A quantum transformation consists of the gate type, target qubit, and optional controls and parameters.

To build a circuit, one or more registers of qubits is initialized, each with a given number of qubits (Appendix B listing 8, line 2). When initializing a circuit, one or more registers of qubits can be used, but only one state structure is defined in the implementation. The `QuantumRegister` facilitates indexing to the intended qubit when writing a circuit. Gate transformations are then added to the circuit using methods of `QuantumCircuit` which include common gate types (Pauli-gates, U -gate), controlled gates and multi-control gates. In Appendix B listing 8, Hadamard (H) gates are added to the circuit on line 6, and Phase (P) gates are added on line 10. For convenience when writing quantum circuits, Spinoza has an inverse quantum Fourier transform function, `iqft`, that can be added to a circuit (or applied to a state) with the same syntax as a single gate application (line 14). The transformations are not applied to the state until the `execute` method is called, as shown in listing 8 line 15. Using the circuit implementation allows for additional optimizations as the order and quantity of gates can be known before execution.

4.2.7 Measurement

We provide a sampling method, `get_samples`, that can be used to simulate measurement results for a given number of shots. Sampling is executed by utilizing weighted reservoir sampling [6]. An example of sampling (using the Python interface) is shown in Appendix C.

4.3 Python Interface

Python is a popular and frequently used programming language in the scientific community. Spinoza can also be used as a Python library to facilitate easy installation and development for users. The Spinoza Python library is designed to be similar to Qiskit to make it easy for researchers to use. The library is implemented using bindings which call Rust code to perform the computations. The Python bindings were implemented using PyO3 [7].

Using Python to call Rust functions adds a negligible overhead. The Python wrapper is used for the benchmarks in figure 6.

5 Optimizations

5.1 Gate Optimizations

5.1.1 X-Gate

$$X = \begin{bmatrix} 0 & 1 \\ 1 & 0 \end{bmatrix}$$

Since the X -gate simply swaps the two sides of the pair, we can completely avoid any arithmetic operations.

When `target = 0`, we have a special case in which `distance = 1`. In this case, we can iterate over the state by stepping by two elements per iteration.

5.1.2 Y-Gate

$$Y = \begin{bmatrix} 0 & -i \\ i & 0 \end{bmatrix}$$

Let the two sides of the pair be γ_0, γ_1 , where $\gamma_0 = a + ib$ and $\gamma_1 = c + id$. The application of the Y -gate to this pair can be expressed as follows:

$$\begin{aligned} Y \begin{bmatrix} \gamma_0 \\ \gamma_1 \end{bmatrix} &= \begin{bmatrix} 0 & -i \\ i & 0 \end{bmatrix} \begin{bmatrix} \gamma_0 \\ \gamma_1 \end{bmatrix} \\ &= \begin{bmatrix} 0 & -i \\ i & 0 \end{bmatrix} \begin{bmatrix} a + ib \\ c + id \end{bmatrix} \\ &= \begin{bmatrix} d - ic \\ -b + ia \end{bmatrix} \end{aligned}$$

We can avoid the extra computations associated with matrix-vector multiplication by noticing that the pair can be “updated” by swapping the vector components, swapping the real and imaginary parts in each component, and by flipping the signs.

In addition, we apply a loop nest optimization (LNO) when using the concatenation strategy. Namely, while appending the target, it is apparent that `((i » target) « target)` rarely changes. Rather, we can explicitly compute the prefixes. As a result, the iteration logic transforms into the following: `base + 0, base + 1, base + 2, ..., base + n`. This transformation presents a vectorization opportunity for the compiler. On the other hand, computing `i + ((i » target) « target)` may cause a jump to something “random”, so the compiler is unable to leverage vectorization.

5.1.3 Z-Gate

$$Z = \begin{bmatrix} 1 & 0 \\ 0 & -1 \end{bmatrix}$$

Let the two sides of the pair be γ_0, γ_1 , where $\gamma_0 = a + ib$ and $\gamma_1 = c + id$. The application of the Z -gate to this pair can be expressed as follows:

$$\begin{aligned}
Z \begin{bmatrix} \gamma_0 \\ \gamma_1 \end{bmatrix} &= \begin{bmatrix} 1 & 0 \\ 0 & -1 \end{bmatrix} \begin{bmatrix} \gamma_0 \\ \gamma_1 \end{bmatrix} \\
&= \begin{bmatrix} 1 & 0 \\ 0 & -1 \end{bmatrix} \begin{bmatrix} a + ib \\ c + id \end{bmatrix} \\
&= \begin{bmatrix} a + ib \\ -c - id \end{bmatrix}
\end{aligned}$$

Given the above result, it is clear that only one side of the pair is needed when applying the Z -gate. Traversing the state while applying the Z -gate will have greater spatial locality as compared to the application of other gates. Namely, regardless of the **target**, the application of the Z -gate will be a cache friendly operation. Thus, we can reduce the number of operations associated with matrix-vector, as well as reduce the required memory bandwidth.

5.1.4 Hadamard Gate

$$H = \begin{bmatrix} \frac{1}{\sqrt{2}} & \frac{1}{\sqrt{2}} \\ \frac{1}{\sqrt{2}} & -\frac{1}{\sqrt{2}} \end{bmatrix}$$

Let the two sides of the pair be γ_0, γ_1 , where $\gamma_0 = a + ib$ and $\gamma_1 = c + id$. The application of the H -gate to this pair can be expressed as follows:

$$\begin{aligned}
H \begin{bmatrix} \gamma_0 \\ \gamma_1 \end{bmatrix} &= \begin{bmatrix} \frac{1}{\sqrt{2}} & \frac{1}{\sqrt{2}} \\ \frac{1}{\sqrt{2}} & -\frac{1}{\sqrt{2}} \end{bmatrix} \begin{bmatrix} \gamma_0 \\ \gamma_1 \end{bmatrix} \\
&= \begin{bmatrix} \frac{1}{\sqrt{2}} & \frac{1}{\sqrt{2}} \\ \frac{1}{\sqrt{2}} & -\frac{1}{\sqrt{2}} \end{bmatrix} \begin{bmatrix} a + ib \\ c + id \end{bmatrix} \\
&= \begin{bmatrix} \frac{a}{\sqrt{2}} + \frac{c}{\sqrt{2}} + i \left(\frac{b}{\sqrt{2}} + \frac{d}{\sqrt{2}} \right) \\ \frac{a}{\sqrt{2}} - \frac{c}{\sqrt{2}} + i \left(\frac{b}{\sqrt{2}} - \frac{d}{\sqrt{2}} \right) \end{bmatrix} \\
&= \begin{bmatrix} (a_1 + c_1) + i(b_1 + d_1) \\ (a_1 - c_1) + i(b_1 - d_1) \end{bmatrix}
\end{aligned}$$

where $a_1 = \frac{a}{\sqrt{2}}, b_1 = \frac{b}{\sqrt{2}}, c_1 = \frac{c}{\sqrt{2}}, d_1 = \frac{d}{\sqrt{2}}$. Hence, we can reduce the number of operations associated with matrix-vector multiplication by taking note of the general structure of applying the Hadamard gate.

5.1.5 Phase Gate

$$P = \begin{bmatrix} 1 & 0 \\ 0 & \cos(\phi) + i \sin(\phi) \end{bmatrix}$$

Let the two sides of the pair be γ_0, γ_1 , where $\gamma_0 = a + ib$ and $\gamma_1 = c + id$. The application of the P -gate to this pair can be expressed as follows:

$$\begin{aligned}
P \begin{bmatrix} \gamma_0 \\ \gamma_1 \end{bmatrix} &= \begin{bmatrix} 1 & 0 \\ 0 & \cos(\phi) + i \sin(\phi) \end{bmatrix} \begin{bmatrix} \gamma_0 \\ \gamma_1 \end{bmatrix} \\
&= \begin{bmatrix} 1 & 0 \\ 0 & \cos(\phi) + i \sin(\phi) \end{bmatrix} \begin{bmatrix} a + ib \\ c + id \end{bmatrix} \\
&= \begin{bmatrix} a + ib \\ c \cos(\phi) - d \sin(\phi) + i(c \sin(\phi) + d \cos(\phi)) \end{bmatrix}
\end{aligned}$$

The Z -gate is a special case of the P -gate, so the P -gate is able to leverage similar optimizations. Namely, the structure of applying on the P -gate to a pair creates an opportunity to avoid the operations associated with the general case of matrix-vector multiplication. Moreover, the P -gate only requires one side of the pair to be modified. Hence, the application of the P -gate allows for greater use of spatial locality.

5.1.6 R_x -Gate

The R_x -gate requires general matrix-vector multiplication, so we leverage fused multiply-add (FMA) instructions to improve the performance of matrix-vector multiplication.

5.1.7 R_y -Gate

Similar to the R_x -gate, the R_y -gate requires general matrix-vector multiplication, so we leverage FMA instructions to improve the performance of matrix-vector multiplication.

5.1.8 R_z -Gate

$$R_z(\lambda) = \begin{bmatrix} e^{-i\frac{\lambda}{2}} & 0 \\ 0 & e^{i\frac{\lambda}{2}} \end{bmatrix}$$

Let the two sides of the pair be γ_0, γ_1 , where $\gamma_0 = a + ib$ and $\gamma_1 = c + id$. The application of the R_z -gate to this pair can be expressed as follows:

$$\begin{aligned}
R_z(\lambda) \begin{bmatrix} \gamma_0 \\ \gamma_1 \end{bmatrix} &= \begin{bmatrix} e^{-i\frac{\lambda}{2}} & 0 \\ 0 & e^{i\frac{\lambda}{2}} \end{bmatrix} \begin{bmatrix} \gamma_0 \\ \gamma_1 \end{bmatrix} \\
&= \begin{bmatrix} e^{-i\frac{\lambda}{2}} & 0 \\ 0 & e^{i\frac{\lambda}{2}} \end{bmatrix} \begin{bmatrix} a + ib \\ c + id \end{bmatrix} \\
&= \begin{bmatrix} a \cos(\frac{\lambda}{2}) + b \sin(\frac{\lambda}{2}) + i(b \cos(\frac{\lambda}{2}) - a \sin(\frac{\lambda}{2})) \\ c \cos(\frac{\lambda}{2}) - d \sin(\frac{\lambda}{2}) + i(c \sin(\frac{\lambda}{2}) + d \cos(\frac{\lambda}{2})) \end{bmatrix}
\end{aligned}$$

Since the R_z matrix is sparse, we can reduce the total number of operations associated with matrix-vector multiplication.

5.1.9 U -Gate

Since the U -gate is the most general single-qubit gate, we leverage FMA instructions to improve the performance of matrix-vector multiplication.

5.2 SIMD

SIMD (Single Instruction Multiple Data) capable CPUs have been available since the introduction of the MMX instruction set [8]. In essence, SIMD operations enable the processing of multiple data with a single instruction. At compile time, Spinoza discerns the CPU type of the local machine, which

allows for the enablement of all instruction subsets supported by the local machine. Modern compilers are able to generate highly optimized series of instructions when provided with simple and predictable code. As such, the loops containing the “fast paths” in the strategies for each gate are manipulated such that the generated code is as long as possible, while only containing low-latency instructions such as `add`, `mul`, etc.

Spinoza’s implementation precludes the need for manual SIMD. The compiler is able to optimize the code given the highly optimized “fast paths”, coupled with the memory layout. The lack of manual SIMD increases the portability of Spinoza. Although manual SIMD can potentially reduce the number of generated, arithmetic, instructions, it is important to note that quantum state simulation is highly memory bound. As a result, the potential savings from handwritten SIMD would not provide any tangible performance benefits. Moreover, use of manual SIMD would necessarily increase the size and complexity of Spinoza due to the need to account for single-precision numbers, double precision numbers, as well as a myriad of architectures.

6 Benchmarks & Comparisons

We compare the performance of Spinoza against several publicly available quantum simulators. We used the public GitHub repository [9], in which benchmarking code has been reviewed by contributors from various libraries. We use the environment setup and configurations as provided in the repository, and compare against the equivalent settings for Spinoza. We used the latest version of each library, as listed in Table 1, unless otherwise specified in the environment setup files provided in the benchmarking repository (i.e. Qiskit). We use Spinoza’s python bindings for a relevant comparison. The implementation of the parameterized quantum circuit used for benchmarking can be found in the repository [9].

Library	Language	Version
Qulacs [10]	C++/Python	0.6.0
ProjectQ [11]	C++/Python	0.8.0
Qiskit [5]	C++/Python	0.16.0
Pennylane [12]	Python	0.30.0
Spinoza	Rust/Python	0.1.0

Table 1: Packages used in benchmarking.

All benchmarks were performed on a `c2-standard-16` instance, with 1 vCPU per core ratio, on Google Cloud Platform (GCP). Spinoza is compiled with `rustc` version 1.67.1, and the following compiler flags: `-C opt-level=3 -C`

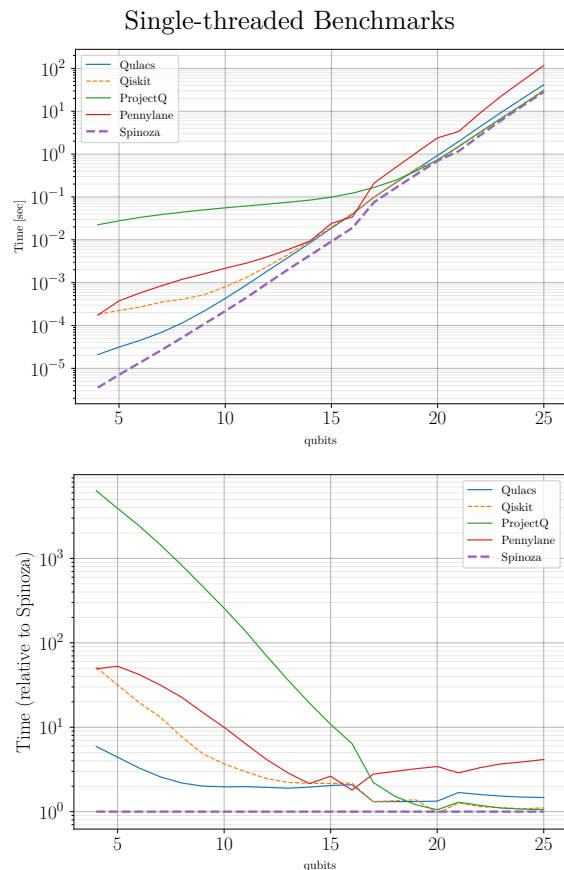


Figure 6: Benchmark times for simulating random quantum circuits, as implemented in [9], using a single thread.

`target-cpu=native -edition=2021`. In addition, we set `codegen-units = 1, lto = true, panic = "abort"`. Lastly, all benchmarks were run using Python 3.8.16.

Additional benchmarks using Spinoza in Rust and Qulacs in C++ are in Appendix D.

6.1 Conclusion and Future Work

Currently, Spinoza is capable of fast quantum state simulation on a myriad of machines when it is only given one thread of execution to leverage. Moreover, Spinoza has an edge over other simulators as shown in Section 6. In future work, Spinoza will be parallelized. In addition, Spinoza will be updated to allow for distributed quantum state simulation.

Acknowledgements

The authors thank Orson R. L. Peters for discussions on code optimization and review. The authors thank Vitaliy Dorum for discussions on design and overall code review.

The views expressed in this article are those of the authors and do not represent the views of Wells

Fargo. This article is for informational purposes only. Nothing contained in this article should be construed as investment advice. Wells Fargo makes no express or implied warranties and expressly disclaims all legal, tax, and accounting implications related to this article.

References

- [1] John Preskill. Quantum computing in the nisq era and beyond. *Quantum*, 2:79, aug 2018. ISSN 2521-327X. DOI: [10.22331/q-2018-08-06-79](https://doi.org/10.22331/q-2018-08-06-79). URL <https://doi.org/10.22331/q-2018-08-06-79>.
- [2] Pixabay License, CCO, free for commercial use, no attribution required, no copyrights apply, 2020. URL <https://pixabay.com/vectors/baruch-spinoza-philosopher-dutch-5689119/>.
- [3] Steve Klabnik and Carol Nichols. *The Rust Programming Language*. No Starch Press, 2019. ISBN 9781718500440.
- [4] 1d or 2d array, what's faster?, 2013. URL <https://stackoverflow.com/a/17260533>.
- [5] Héctor Abraham et al. Qiskit: An open-source framework for quantum computing, 2019. URL <https://doi.org/10.5281/zenodo.2562110>.
- [6] Benedikt Bitterli, Chris Wyman, Matt Pharr, Peter Shirley, Aaron Lefohn, and Wojciech Jarosz. Spatiotemporal reservoir resampling for real-time ray tracing with dynamic direct lighting. *ACM Trans. Graph.*, 39(4), aug 2020. ISSN 0730-0301. DOI: [10.1145/3386569.3392481](https://doi.org/10.1145/3386569.3392481). URL <https://doi.org/10.1145/3386569.3392481>.
- [7] David Hewitt et al. Pyo3. URL <https://pyo3.rs/v0.16.4/index.html>.
- [8] Intel intrinsics guide, 2022. URL <https://www.intel.com/content/www/us/en/docs/intrinsics-guide/index.html>.
- [9] Xiu-Zhe (Roger) Luo and contributors. Quantum software benchmarks. URL <https://github.com/yardstick/quantum-benchmarks>.
- [10] Yasunari Suzuki, Yoshiaki Kawase, Yuya Masumura, Yuria Hiraga, Masahiro Nakadai, Jiabao Chen, Ken M. Nakanishi, Kosuke Mitarai, Ryosuke Imai, Shiro Tamiya, Takahiro Yamamoto, Tennin Yan, Toru Kawakubo, Yuya O. Nakagawa, Yohei Ibe, Youyuan Zhang, Hirotsugu Yamashita, Hikaru Yoshimura, Akihiro Hayashi, and Keisuke Fujii. Qulacs: a fast and versatile quantum circuit simulator for research purpose. *Quantum*, 5:559, October 2021. ISSN 2521-327X. DOI: [10.22331/q-2021-10-06-559](https://doi.org/10.22331/q-2021-10-06-559). URL <https://doi.org/10.22331/q-2021-10-06-559>.
- [11] Damian S. Steiger, Thomas Häner, and Matthias Troyer. ProjectQ: an open source software framework for quantum computing. *Quantum*, 2:49, January 2018. ISSN 2521-327X. DOI: [10.22331/q-2018-01-31-49](https://doi.org/10.22331/q-2018-01-31-49). URL <https://doi.org/10.22331/q-2018-01-31-49>.
- [12] Ville Bergholm, Josh Izaac, Maria Schuld, Christian Gogolin, Shahnawaz Ahmed, Vishnu Ajith, M. Sohaib Alam, Guillermo Alonso-Linaje, B. AkashNarayanan, Ali Asadi, Juan Miguel Arrazola, Utkarsh Azad, Sam Banning, Carsten Blank, Thomas R Bromley, Benjamin A. Cordier, Jack Ceroni, Alain Delgado, Olivia Di Matteo, Amintor Dusko, Tanya Garg, Diego Guala, Anthony Hayes, Ryan Hill, Aroosa Ijaz, Theodor Isacsson, David Ittah, Soran Jahangiri, Prateek Jain, Edward Jiang, Ankit Khandelwal, Korbinian Kottmann, Robert A. Lang, Christina Lee, Thomas Loke, Angus Lowe, Keri McKiernan, Johannes Jakob Meyer, J. A. Montañez-Barrera, Romain Moyard, Zeyue Niu, Lee James O'Riordan, Steven Oud, Ashish Panigrahi, Chae-Yeun Park, Daniel Polatajko, Nicolás Quesada, Chase Roberts, Nahum Sá, Isidor Schoch, Borun Shi, Shuli Shu, Sukin Sim, Arshpreet Singh, Ingrid Strandberg, Jay Soni, Antal Száva, Slimane Thabet, Rodrigo A. Vargas-Hernández, Trevor Vincent, Nicola Vitucci, Maurice Weber, David Wierichs, Roeland Wiersema, Moritz Willmann, Vincent Wong, Shaoming Zhang, and Nathan Killoran. PennyLane: Automatic differentiation of hybrid quantum-classical computations, 2018. URL <https://arxiv.org/abs/1811.04968>.
- [13] Charlee Stefanski, Vanio Markov, and Constantin Gonciulea. Quantum amplitude interpolation, 2022. URL <https://arxiv.org/abs/2203.08758>.

A Data Structures and Pair Strategies in Rust

```
1 pub struct State {
2     pub reals: Vec<Float>,
3     pub imgs: Vec<Float>,
4     pub n: u8,
5 }
```

Listing 1: State structure definition. Float can be type f32 or f64—depending on the feature flag chosen.

```

1 for i in 0..(1 << state.n) {
2     let k = (i >> target) & 1;
3     let m = &self.m[k];
4     // UPDATE AMPLITUDES
5 }

```

Listing 2: Rust implementation Strategy 0 - Traverse and Recognize.

```

1 let mut chunk_start = range.start;
2
3 while chunk_start < range.end {
4     let chunk_end = range.end.min(((chunk_start >> target) + 1) << target);
5
6     let m = self.matrix[(chunk_start >> target) & 1];
7     for i in chunk_start..chunk_end {
8         // UPDATE AMPLITUDES
9     }
10    chunk_start = chunk_end;
11 }

```

Listing 3: Rust implementation Strategy 1 - Group and Traverse.

```

1 let end = state.imags.len() >> 1;
2 let chunks = end >> target;
3
4 (0..chunks).into_iter().for_each(|chunk| {
5     let dist = 1 << target;
6     let base = (2 * chunk) << target;
7     for i in 0..dist {
8         let l0 = base + i;
9         let l1 = l0 + dist;
10        // UPDATE AMPLITUDES
11    }
12 })

```

Listing 4: Rust implementation of Strategy 2 - Concatenation.

```

1 let dist = 1 << target;
2 let num_pairs = state.len() >> 1;
3
4 for i in 0..num_pairs {
5     let l0 = i + ((i >> target) << target);
6     let l1 = l0 + dist;
7     // UPDATE AMPLITUDES
8 }

```

Listing 5: Rust implementation of Strategy 3 - Insertion.

```

1 let end = state.imags.len() >> 2;
2
3 let dist = 1 << target;
4 let marks = (target.min(control), target.max(control));
5
6 for i in 0..end {
7     let x = i + (1 << (marks.1 - 1)) + ((i >> (marks.1 - 1)) << (marks.1 - 1));
8     let l1 = x + (1 << marks.0) + ((x >> marks.0) << marks.0);
9     let l0 = l1 - dist;
10    // UPDATE AMPLITUDES
11 }

```

Listing 6: Rust implementation of Strategy 3 - Insertion, for controlled gate transformations.

B Using Spinoza: Rust

```

1 fn value_encoding(n: usize, v: Float) {
2     let mut state = State::new(n);
3
4     for i in 0..n {
5         apply(Gate::H, &mut state, i);
6     }
7
8     for i in 0..n {

```

```

9     apply(Gate::P(2.0 * PI / (pow2f(i + 1)) * v), &mut state, i);
10 }
11
12 let targets: Vec<usize> = (0..n).rev().collect();
13 iqft(&mut state, &targets);
14 }

```

Listing 7: Value Encoding, as described in [13], implemented using Spinoza.

```

1 fn value_encoding(n: usize, v: Float) {
2     let mut q = QuantumRegister::new(n);
3     let mut qc = QuantumCircuit::new(&mut q);
4
5     for i in 0..n {
6         qc.h(q[i])
7     }
8
9     for i in 0..n {
10        qc.p((2 as Float) * PI / pow2f(i + 1) * v, q[i])
11    }
12
13    let targets: Vec<usize> = (0..n).rev().collect();
14    qc.iqft(&targets);
15
16    qc.execute();
17 }

```

Listing 8: Value Encoding circuit, as described in [13], implemented using Spinoza.

C Using Spinoza: Python

```

1 def value_encoding(n, v):
2     q = QuantumRegister(n)
3     qc = QuantumCircuit(q)
4
5     for i in range(n):
6         qc.h(i)
7
8     for i in range(n):
9         qc.p(2 * np.pi / (2 ** (i + 1)) * v, i)
10
11    qc.iqft(range(n)[::-1])
12
13    return qc

```

Listing 9: Value Encoding circuit, as described in [13], implemented using the Spinoza Python Library.

```

1 circuit = value_encoding(3, 2.4)
2 state = run(circuit)
3
4 samples = get_samples(state, 1000)

```

Listing 10: Using the resulting statevector from running the value encoding circuit defined in listing 9 on three qubits with the parameter 2.4 we get 1,000 samples using reservoir sampling

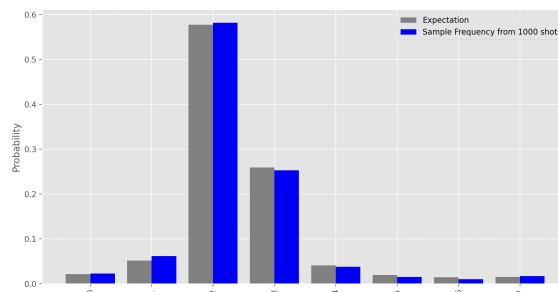


Figure 7: Expected probabilities versus sample frequencies from the state and samples in listing 10.

D Rust Benchmarks

The following benchmarks were implemented using the Rust implementation of Spinoza and the C++ implementation of Qulacs. This allows for comparison without concern for the overhead from using the respective Python libraries.

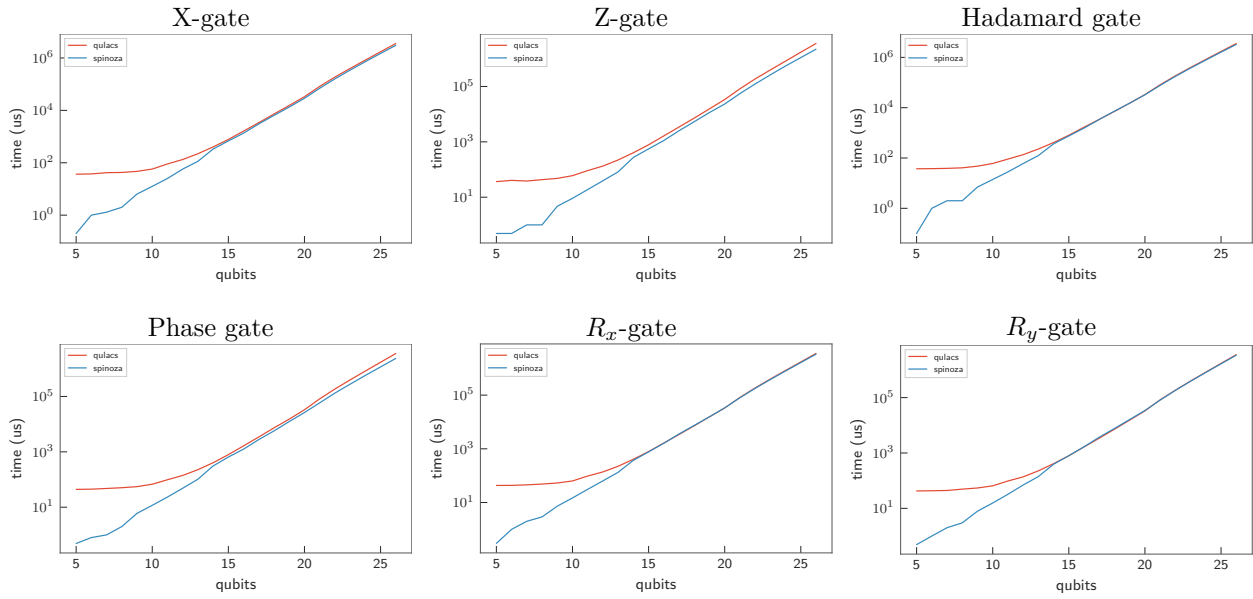


Figure 8: Average time (logarithmic scale) to execute ten iterations of applying the given gate to each qubit in a system for five to twenty-six qubits.

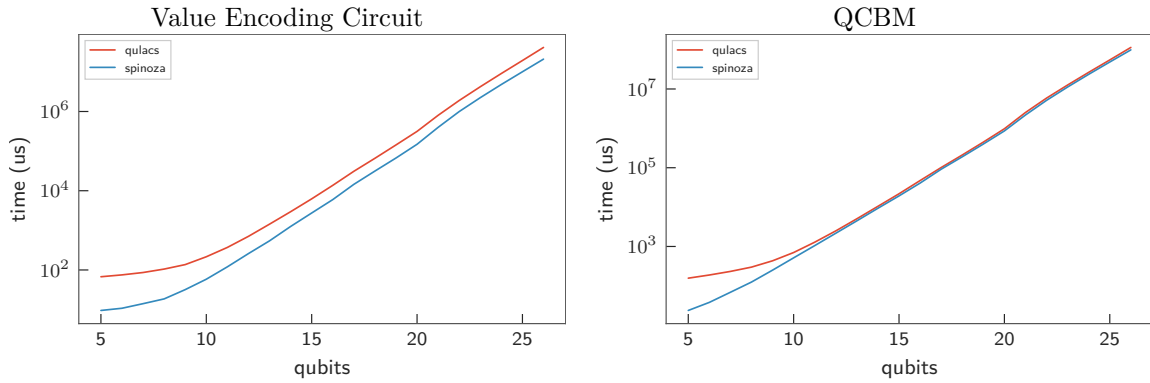


Figure 9: Average time (logarithmic scale) to execute ten iterations of the "QCBM" quantum circuits (as implemented in [9]) for five to twenty-six qubits.